

BAX inhibitor-1 regulates autophagy by controlling the IRE1 α branch of the unfolded protein response

Karen Castillo^{1,2}, Diego Rojas-Rivera^{1,2},
Fernanda Lisboa^{1,2}, Benjamín Caballero^{1,2},
Melissa Nassif^{1,2}, Felipe A Court³,
Sebastian Schuck⁴, Consuelo Ibar⁵,
Peter Walter⁴, Jimena Sierralta²,
Alvaro Glavic⁵ and Claudio Hetz^{1,2,6,*}

¹Center for Molecular Studies of the Cell, Department of Cellular and Molecular Biology, Institute of Biomedical Sciences, University of Chile, Santiago, Chile, ²Biomedical Neuroscience Institute, Faculty of Medicine, University of Chile, Santiago, Chile, ³Millennium Nucleus for Regenerative Biology, Department of Physiological Sciences, Faculty of Biology, P. Catholic University of Chile, Santiago, Chile, ⁴Howard Hughes Medical Institute and Department of Biochemistry and Biophysics, University of California at San Francisco, San Francisco, CA, USA, ⁵Center for Genome Regulation, Department of Biology, Faculty of Sciences, University of Chile, Santiago, Chile and ⁶Department of Immunology and Infectious Diseases, Harvard School of Public Health, Boston, MA, USA

Both autophagy and apoptosis are tightly regulated processes playing a central role in tissue homeostasis. Bax inhibitor 1 (BI-1) is a highly conserved protein with a dual role in apoptosis and endoplasmic reticulum (ER) stress signalling through the regulation of the ER stress sensor inositol requiring kinase 1 α (IRE1 α). Here, we describe a novel function of BI-1 in the modulation of autophagy. BI-1-deficient cells presented a faster and stronger induction of autophagy, increasing LC3 flux and autophagosome formation. These effects were associated with enhanced cell survival under nutrient deprivation. Repression of autophagy by BI-1 was dependent on cJun-N terminal kinase (JNK) and IRE1 α expression, possibly due to a displacement of TNF-receptor associated factor-2 (TRAF2) from IRE1 α . Targeting BI-1 expression in flies altered autophagy fluxes and salivary gland degradation. BI-1 deficiency increased flies survival under fasting conditions. Increased expression of autophagy indicators was observed in the liver and kidney of *bi-1*-deficient mice. In summary, we identify a novel function of BI-1 in multicellular organisms, and suggest a critical role of BI-1 as a stress integrator that modulates autophagy levels and other interconnected homeostatic processes.

The EMBO Journal (2011) 30, 4465–4478. doi:10.1038/emboj.2011.318; Published online 16 September 2011
Subject Categories: signal transduction; differentiation & death

*Corresponding author. Department of Immunology and Infectious Diseases, Harvard School of Public Health, Boston, MA 02115, USA or Independencia 1027, Faculty of Medicine, Institute of Biomedical Sciences, University of Chile, Santiago, Chile.
Tel.: +56 2 9786506; Fax: +56 2 9786871;
E-mail: chetz@med.uchile.cl or chetz@hsph.harvard.edu

Received: 31 January 2011; accepted: 1 August 2011; published online: 16 September 2011

Keywords: autophagy; bax inhibitor-1(BI-1); inositol requiring kinase 1 α (IRE1 α); jun-terminal kinase (JNK); microtubule-associated protein 1 light chain 3 (LC3)

Introduction

Macroautophagy, here referred to as autophagy, is a highly conserved and regulated process involved in the catabolism of cytoplasmic components that are recycled to maintain energy production and macromolecule synthesis. Autophagy involves the encapsulation of cargoes into double-membrane vesicles (autophagosome), which fuse with lysosomes forming the autolysosomes where cargoes are degraded (Levine and Kroemer, 2008). Under nutrient starvation, autophagy maintains energy homeostasis, but it also regulates tissue remodelling during development, and catalyses the removal of harmful or superfluous cellular organelles, aggregation-prone proteins, and intracellular pathogens (Mizushima *et al.*, 2008; He and Klionsky, 2009). Furthermore, emerging evidence indicates that altered autophagy also contributes to a number of inflammatory and neurodegenerative diseases, in addition to cancer and diabetes (Levine and Kroemer, 2008; Wong and Cuervo, 2010).

Autophagy-related (ATG) genes regulate different sequential steps in the autophagy process (Maiuri *et al.*, 2007b; He and Klionsky, 2009), starting with the formation of a protein kinase-autophagy regulatory complex and a lipid kinase-signalling complex. ATG proteins, including a class III PI-3-kinase complex, are involved in vesicle nucleation, which is positively regulated by Beclin-1 (He and Levine, 2010). A key event in autophagosome formation is the conversion of microtubule-associated protein 1 light chain 3 (LC3-I) into the LC3-II form through its lipidation. Monitoring LC3 flux through the autophagolysosomal pathway is the current gold standard to monitor autophagy activity (Klionsky *et al.*, 2008; Tanida *et al.*, 2008). A complex inter-relationship operates between autophagy and apoptosis signalling pathways, where the BCL-2 protein family plays a central role in mediating the cross talk of both processes (Hetz and Glimcher, 2008; Wei *et al.*, 2008b; Pattingre *et al.*, 2009; Chen and Debnath, 2010). For example, the anti-apoptotic BCL-2 and BCL-X_L proteins negatively regulate autophagy by binding to and inhibiting Beclin-1 (Pattingre *et al.*, 2005). Pro-apoptotic BH3-only proteins (Maiuri *et al.*, 2007a) or BCL-2 phosphorylation by cJun-N terminal kinase (JNK; Pattingre *et al.*, 2009) antagonize BECLIN-1/BCL-2 interactions, enhancing autophagy. This autophagy regulatory network is proposed to operate at the endoplasmic reticulum (ER) membrane (Pattingre *et al.*, 2005). Although the BCL-2 family of proteins has an essential role in apoptosis and autophagy in mammals and *C. elegans*, the function of these proteins in

other model organisms where autophagy is physiologically relevant, such as fly and yeast, is not clear. This is based on the fact that BCL-2 family homologues have not been described in yeast and that the two BCL-2 family members identified in *Drosophila melanogaster* (BCL-2/Buffy and BAX/Debcl) have unclear roles in programmed cell death (Sevrioukov *et al*, 2007; Galindo *et al*, 2009). Furthermore, their apoptosis activities are restricted to specific conditions (Quinn *et al*, 2003; Wu *et al*, 2010). Interestingly, a genetic screening using a fly cell line identified Debcl and Buffy as possible pro-autophagy regulators (Hou *et al*, 2008).

Bax inhibitor-1 (BI-1), also known as *transmembrane BAX inhibitor motif containing 6* (TMBIM6), is a highly conserved cell death regulator and its sequence is present in mammals, insects, plants, yeasts, viruses, and other species (Chae *et al*, 2003; Huckelhoven, 2004; Reimers *et al*, 2008). BI-1 is an ER-located protein containing six transmembrane regions with anti-apoptotic functions, involved in the suppression of intrinsic cell death mediated by ER calcium release (Xu and Reed, 1998; Xu *et al*, 2008), ER stress (Chae *et al*, 2004; Lisbona *et al*, 2009), and ischaemia (Bailly-Maitre *et al*, 2006; Dohm *et al*, 2006; Krajewska *et al*, 2011). At the mechanistic level, BI-1 has been shown to influence the steady state of ER calcium levels (Westphalen *et al*, 2005; Kim *et al*, 2008; Xu *et al*, 2008; Ahn *et al*, 2010). BI-1 inhibits the activity of the ER stress sensor inositol requiring kinase 1 α (IRE1 α) by a direct interaction (Lisbona *et al*, 2009; Bailly-Maitre *et al*, 2010). Interestingly, ER stress is a particularly efficient stimulus for autophagy (Hoyer-Hansen and Jaattela, 2007). ER stress is caused by the accumulation of incorrectly folded proteins in the ER lumen, engaging an adaptive reaction known as the unfolded protein response (UPR) (Hetz and Glimcher, 2009). In mammals, the UPR signals through the activation of three transmembrane proteins where IRE1 α is the most conserved stress sensor (Ron and Walter, 2007). IRE1 α is a kinase/endoribonuclease that, upon activation, initiates the splicing of the mRNA encoding the transcription factor X-Box-binding protein 1 (XBP-1), converting it into a potent activator of UPR target genes (Hetz and Glimcher, 2009). IRE1 α also regulates autophagy levels during ER stress by binding to the adaptor protein TNF-receptor associated factor-2 (TRAF2), followed by the downstream activation of JNK (Ogata *et al*, 2006; Ding *et al*, 2007). XBP-1 levels could also modulate autophagy in mammals and fly cells (Arsham and Neufeld, 2009; Hetz *et al*, 2009). In this study, we have identified a new function of the evolutionary conserved protein BI-1 in the control of autophagy. Our results indicate that BI-1 negatively modulates the kinetics and amplitude of autophagy fluxes in cells undergoing nutrient starvation. BI-1 expression controlled autophagy by regulating JNK activation, possibly due to a mechanism involving IRE1 α and TRAF2. This study may give additional clues about the physiological integration between apoptosis and autophagy in different species.

Results

BI-1 deficiency leads to accumulation of acidic vesicles and autophagosomes

To explore the possible impact of BI-1 on the lysosomal pathway, we first visualized the content of acidic compartments using lysotracker staining in BI-1 wild-type (WT) and deficient (KO) mouse embryonic fibroblasts (MEFs). We also

monitor ER morphology expressing a Cytochrome b5-EGFP fusion protein. Unexpectedly, augmented number of acidic vesicles with larger size was observed in BI-1-deficient cells cultured in standard media (Figure 1A). In contrast, the distribution pattern of the ER network in BI-1 WT and KO cells was similar under this condition, suggesting a specific effect on acidic compartments (Figure 1A).

Recent reports indicate that autophagy involves enhanced lysosome biogenesis (Settembre *et al*, 2011) and redistribution (Korolchuk *et al*, 2011). We exposed cells to nutrient starvation to induce autophagy by incubations in Earle's Balanced Salt Solution (EBSS) or serum/glucose-free RPMI media. These treatments led to a stronger redistribution and accumulation of large acidic vesicles in BI-1 KO cells when compared with WT control cells (Figure 1B), an effect reverted by reconstituting cells with a BI-1-GFP expression vector (Supplementary Figure S1A). Then, we analysed the morphology of these acidic vesicles by electron microscopy (EM) using the combined colocalization between fluorescence and EM images. A low magnification of BI-1 KO MEFs cells subjected to nutrient starvation and stained with lysotracker is shown in Figure 1C (panels *a-e*) (see also Supplementary Figure S1B and C). Ultrastructural EM analysis of the larger lysotracker-positive vacuoles revealed the appearance of vesicular structures with distinct characteristics, including multivesicular membranes (Figure 1C, panel *f*), lysosomes with intracellular content (Figure 1C, panel *g*), and late stage autophagy vesicles which accumulated in clusters (Figure 1C, panel *h*), which is an indirect indicative of enhanced autophagy (Korolchuk *et al*, 2011). To directly monitor the possible impact of BI-1 on autophagosome formation, we then visualized the presence of LC3-positive vesicles in cells cultured in standard media or after nutrient starvation. Increased accumulation of LC3-positive dots, that also present dots of higher size, was observed in BI-1 KO cells compared with control cells in both conditions (Figure 1D).

BI-1 deficiency enhances the kinetic and amplitude of autophagy flux

The accumulation of autophagosomes in BI-1-deficient cells could have two paradoxical interpretations: increased autophagy activity or impaired fusion of autophagosome vesicles, decreasing their flow through the autophagy pathway. Thus, we performed LC3-II flux assays using inhibitors of lysosomal activity and western blot analysis. First of all, we monitored in kinetic experiments the levels of LC3-II in BI-1 WT and KO cells under resting or nutrient starvation conditions (Figure 2A). Quantification revealed a faster induction of LC3-II in BI-1-deficient cells (0–1 h) in relation to a loading control after stimulation with EBSS or with serum/glucose-free RPMI media (Figure 2B). In addition, an ~2.5-fold increase in LC3-II levels was observed after 3 h of nutrient starvation compared with control cells (Figure 2B). Although, a slight upregulation of LC3-I form was observed, no changes on *lc3* mRNA levels were detected in BI-1-deficient cells by real-time PCR compared with control cells (Supplementary Figure S1D).

We then measured LC3-II flux through the autophagy pathway by exposing cells to nutrient deprivation in the presence or absence of a cocktail of lysosomal inhibitors (200 nM bafilomycin A₁, 10 μ g/ml pepstatin and 10 μ g/ml E64d). A further accumulation of LC3-II in BI-1-deficient

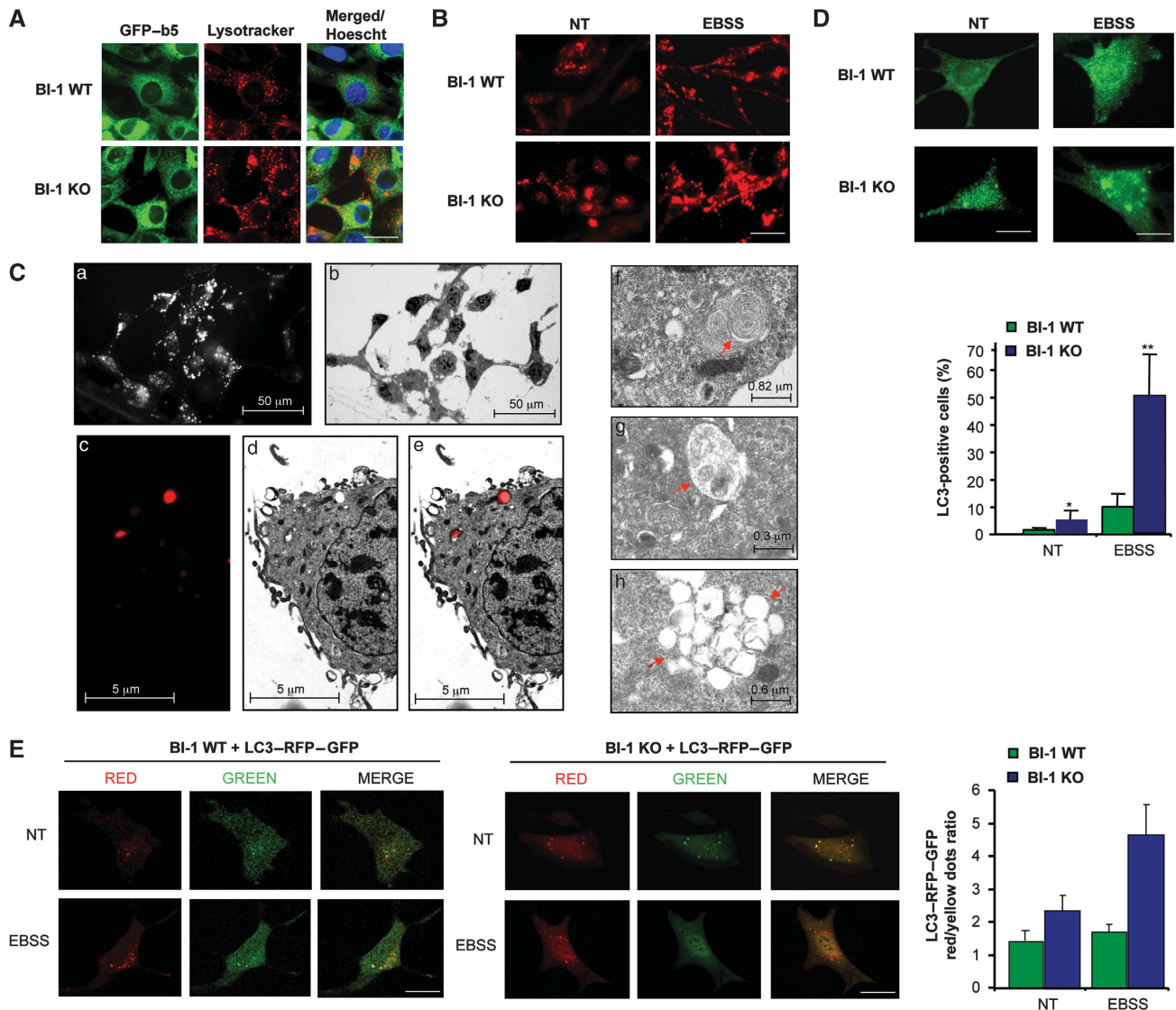


Figure 1 Increased accumulation of autophagosomes and lysosomes in BI-1-deficient cells. (A) BI-1 WT and KO MEFs cells were stably transduced with retroviruses expressing cytochrome b5-GFP to visualize the ER (green). Then cells were stained with lysotracker (red) and observed with a confocal microscope. Nucleus was stained with Hoechst (blue). Scale bar: 30 μm . (B) BI-1 WT and KO MEFs cells stimulated with EBSS for 3 h to induce autophagy. Acidic vesicles were visualized with a confocal microscope after lysotracker staining. Data represent the results of three independent experiments. Scale bar: 50 μm . (C) (a) Epifluorescence imaging of BI-1 KO cells stained with lysotracker; (b) electron micrograph of the same field of cells shown in (a); (c-e), magnification of lysotracker-positive vesicles in BI-1 KO cells exposed to EBSS for 3 h and visualized with a fluorescent microscope (c) and the same field subsequently imaged by EM (d). Overlapping images are presented (e). Left panel: analysis of vesicular structures by EM with morphologies resembling early (f), intermediate (g) and late (h) autophagy vesicles. (D) Left panel: the distribution of endogenous LC3 was monitored by immunofluorescence and confocal microscopy in BI-1 WT and KO MEFs cells at basal conditions (NT) or after exposure to EBSS for 3 h. Scale bar: left 15 μm and right 10 μm . Right panel: quantification of the number cells containing three or more LC3-positive vesicles ($N = 160$ cells). Mean and standard deviation are presented ($N = 4$). Student's t -test was used to analyse statistical significance, $**P < 0.001$ and $*P < 0.01$. (E) BI-1 WT and KO cells were transiently transfected with an expression vector for a monomeric-tandem LC3-RFP-GFP construct. After 24 h, cells were exposed to EBSS for 3 h. Autophagy fluxes were monitored in living cells by visualizing the distribution of LC3-positive dots in the red and green channels using a confocal microscope. Scale bar: 10 μm . Right panel: quantification of the ratio between red and yellow dots per cell is presented. Mean and standard error of the analysis of 15 cells are shown.

cells was observed when lysosomal activity was inhibited (Figure 2C and D), indicating enhanced autophagy activity in the absence of BI-1. In addition, blocking PI3K by the treatment with 10 mM 3-methyladenine (3-MA) abrogated the accumulation of LC3-II in cells undergoing nutrient starvation (Figure 2C and D). Taken together, these data suggest that BI-1 negatively controls the magnitude and the kinetic of autophagy in response to starvation. As shown in Figure 2A, we also observed a slight accumulation of LC3-II in BI-1 KO

cells grown in normal cell culture media. This prompts us to perform an LC3 flux assay in the presence of nutrients. A higher accumulation of LC3-II was observed in BI-1 KO cells compared with control cells after inhibition of lysosomal activity under this condition (Figure 2E), implying enhanced basal autophagy levels in cells lacking BI-1. Finally, as additional control, we reconstituted BI-1 KO cells using retroviruses to express BI-1^{WT}-GFP, which as expected reduced LC3-II levels in these cells after nutrient starvation (Figure 2F).

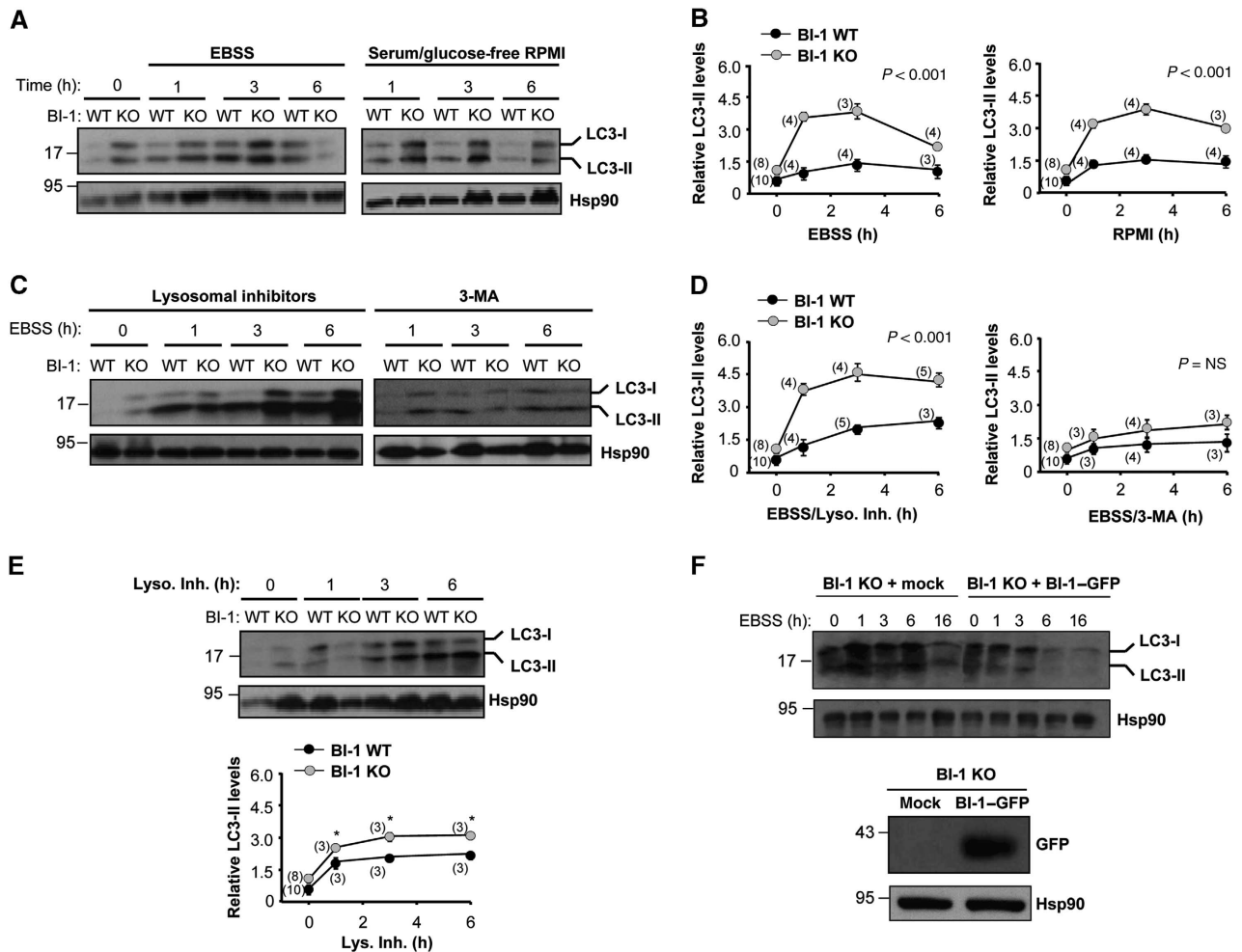


Figure 2 BI-1 deficiency enhances autophagy flux. (A) BI-1 WT and KO MEFs were treated with EBSS (left panel) or glucose/serum-free RPMI media (right panel) for the indicated time points. Then, levels of LC3 were determined by western blot analysis. LC3-I and LC3-II forms are indicated. Hsp90 levels were assessed as loading control. (B) Quantification of LC3-II levels relative to Hsp90 expression was performed in several experiments performed as presented in (A). (C) Cells were pre-treated with a cocktail of lysosomal inhibitors (200 nM bafilomycin A₁, 10 µg/ml pepstatin, and E64d; left panel) or 10 mM 3-methyladenine (3-MA; right panel) for 12 h and then exposed to starvation. LC3 levels monitored by western blot (D) and quantification of LC3-II levels relative to Hsp90 were performed in the experimental conditions described in (C). (E) Basal autophagy flux was monitored in cells treated with a cocktail of lysosomal inhibitors (Lys. Inh.) in the presence of normal cell culture media. Right panel: quantification of independent experiments is presented. (F) BI-1 KO cells were stably transduced with retroviruses expressing BI-1-GFP or empty vector, and then levels of LC3-II were assessed over time by western blot analysis after exposure to EBSS. Right panel: as control, the levels of BI-1-GFP were monitored by western blot. Hsp90 levels were used as loading control. In (B, D and E) mean and standard deviation are presented. Two-way ANOVA was applied to analyse statistical significance. In parenthesis, the number of independent experiments for each time point is indicated. Student's *t*-test was also used in (E) to analyse the statistical significance between each time point (**P* < 0.001). In (B, D and E), normalization was performed as a ratio with the LC3-II/Hsp90 normalized levels from non-treated BI-1 WT cells.

To examine autophagy flux in the absence of lysosomal inhibitors, we transiently expressed a tandem monomeric LC3-RFP-GFP construct (Klionsky *et al*, 2008) in BI-1 WT and KO MEFs. Using this dynamic autophagy sensor, we detected a large accumulation of LC3-red dots in BI-1 KO cells undergoing nutrient starvation, which is indicative of a flux of LC3 from autophagosomes (colocalization RFP and GFP) to autophagolysosomes (quenched GFP signal by acidic lysosomal environment) (Figure 1E). Colocalization of EM images with fluorescent images confirmed the presence of autophagolysosomes vesicles in BI-1 KO cells (Supplementary Figure S1E).

Additionally, we monitored the flux of the autophagy substrate p62/SQSTM1 during the starvation period. Although a slight increase in basal p62/SQSTM1 expression was observed in BI-1 KO cells by western blot analysis, enhanced p62/SQSTM1

degradation was detected under conditions of nutrient starvation over time (Supplementary Figure S2A, B and D), and confirmed by immunofluorescence analysis of p62/SQSTM1 distribution (Supplementary Figure S2C).

BI-1 deficiency improves cell survival under nutrient starvation conditions

To functionally address the cellular consequences of augmented autophagy in BI-1-deficient cells, we determined the rate of cell survival under nutrient starvation using several complementary assays. We first monitored relative cell number with the MTS assay over time. After exposing cells to EBSS, we observed enhanced viability of BI-1 KO cells compared with control cells (Figure 3A, left panel). In sharp contrast, BI-1-deficient cells were more susceptible to ER stress-induced apoptosis triggered by different concen-

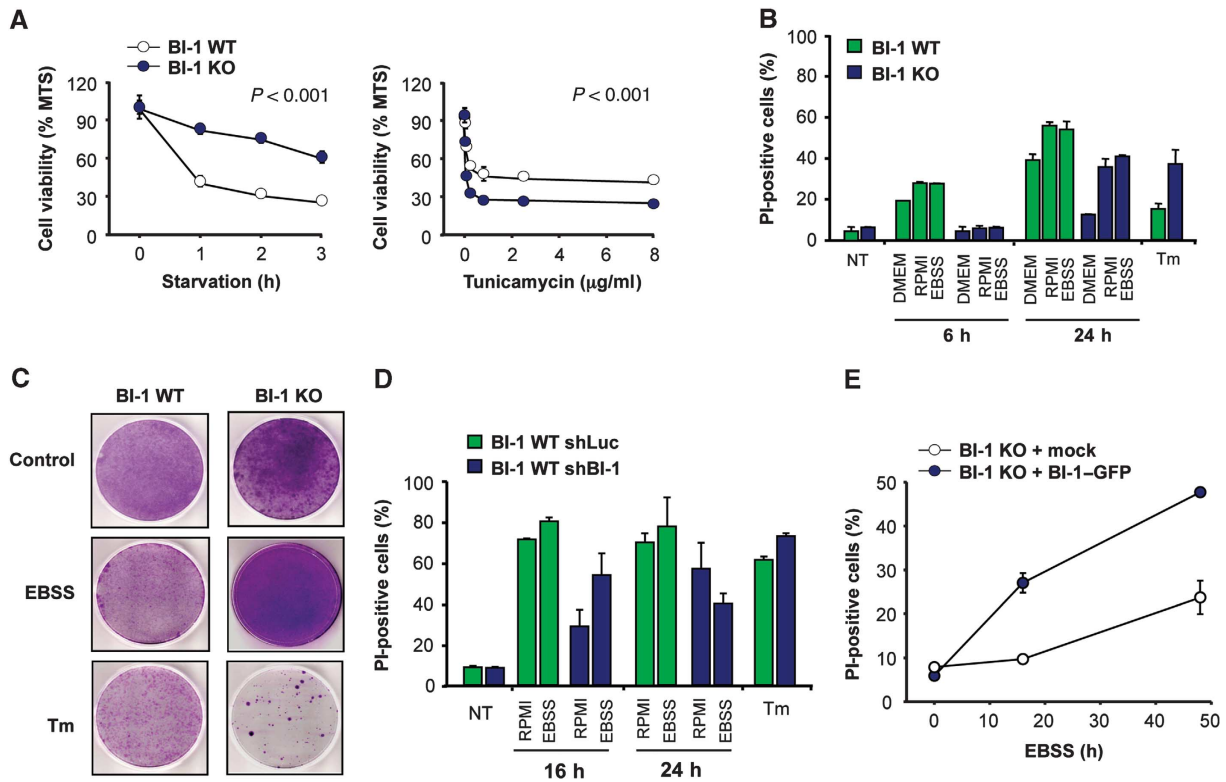


Figure 3 BI-1 deficiency increases cell survival under nutrient starvation conditions. (A) Left panel: BI-1 WT and KO MEFs cells were incubated in EBSS, and then cell viability was monitored using the MTS assay. Right panel: a similar experiment was performed after treating cells with the indicated concentration of tunicamycin for 24 h. Mean and standard deviation are presented of triplicates representative of three independent experiments. (B) BI-1 WT and KO cells were treated with three different starvation stimuli for 6 and 24 h. Cell death was determined after propidium iodide (PI) staining and FACS analysis. In addition, cells were treated with 100 ng/ml tunicamycin (Tm) for 24 h. Mean and standard deviation are presented of one experiment performed in triplicates. (C) Cells were exposed to EBSS for 6 h or 1 $\mu\text{g/ml}$ Tm for 2 h, and then replated in normal cell culture media. After 5 days, cell viability was monitored by staining with crystal violet. Data are representative of three independent experiments. (D) BI-1 WT MEFs were stably transduced with lentiviral expression vectors to deliver an shRNA against *bi-1* mRNA or control mRNA (*luciferase* shRNA). Cell survival was measured after treatment of cells as described in (B). Mean and standard deviation of an experiment made by triplicate, representative of two independent experiments. (E) BI-1 KO cells were stably transduced with retroviruses expressing BI-1-GFP or empty vector, and then exposed to EBSS for indicated time points. Cell viability was monitored after PI staining by FACS. Mean and standard deviation are presented of triplicates representative of two independent experiments.

trations of tunicamycin (Figure 3A, right panel), consistent with previous reports describing a downstream regulation of the apoptosis machinery (Chae *et al*, 2004; Bailly-Maitre *et al*, 2006).

We then quantified the levels of cell death using propidium iodide (PI) staining and FACS analysis. By stimulating with three different conditions of nutrient starvation, we detected a dramatic protection of BI-1 KO cells after 6 h of treatment (Figure 3B). These effects were observed even after prolonged starvation (24 h of treatment, Figure 3B). Again, treatment of cells with the ER stress agent tunicamycin led to enhanced cell death of BI-1-deficient cells when compared with control WT cells (Figure 3B). Then, we monitored the ability of cells to adapt to nutrient starvation using transient exposure to the stimuli and a replating assay. Using this method, we observed a higher ability of BI-1-deficient cells to survive under nutrient starvation conditions (Figure 3C), which contrasted with their high susceptibility to tunicamycin treatment. Finally, to confirm these results, we knocked down the expression of BI-1 in WT cells using shRNA and stable lentiviral transduction. This strategy leads to a decrease of $\sim 75\%$ of the *bi-1* mRNA levels monitored by real-time PCR (not shown) as described before (Lisbona

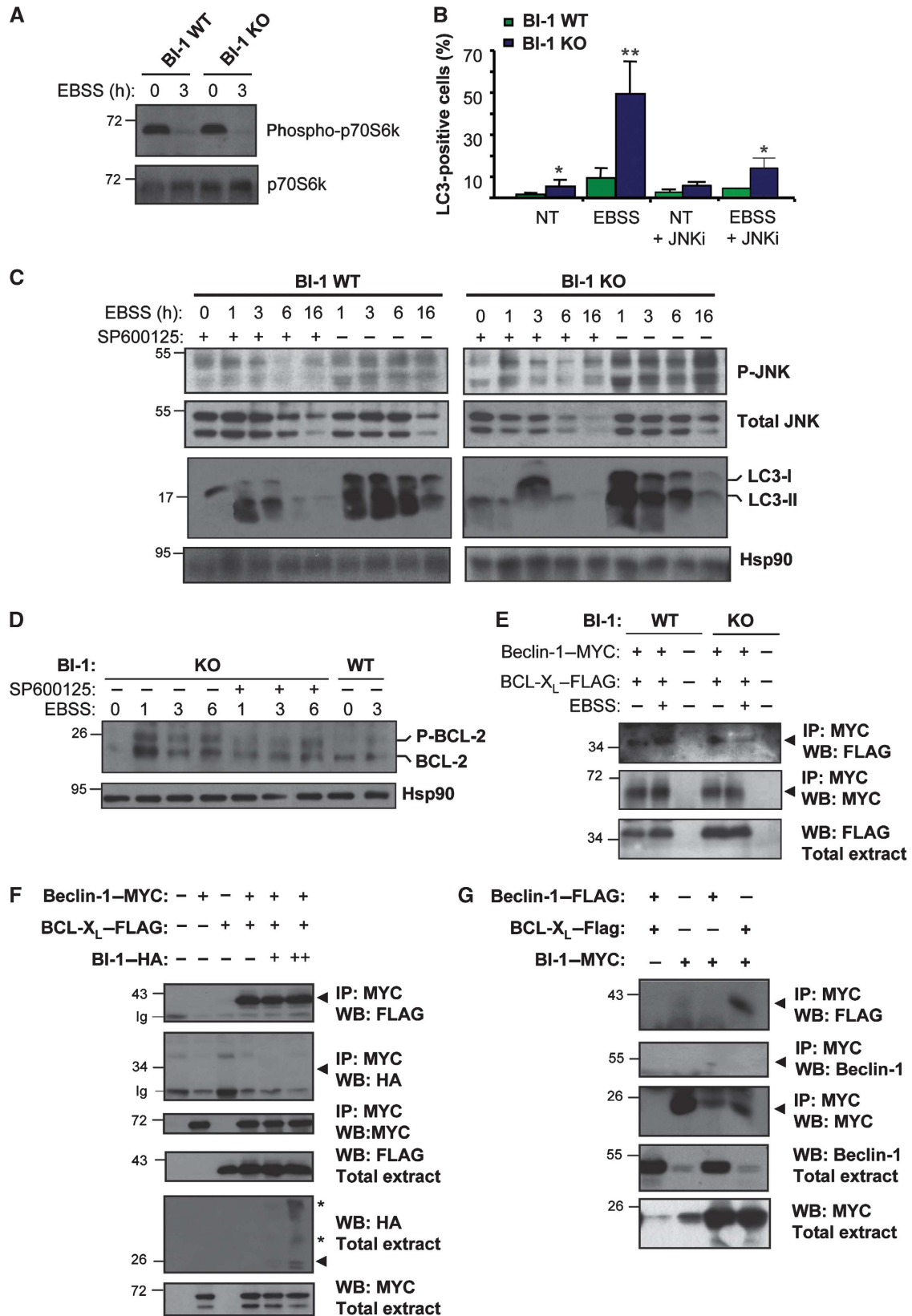
et al, 2009). Targeting *bi-1* partially protected cells against nutrient starvation, and slightly enhanced the susceptibility to tunicamycin toxicity (Figure 3D). We also stably over-expressed BI-1-GFP using retroviral transduction in BI-1 KO MEFs and then monitored the susceptibility of these cells to nutrient starvation (Figure 3E). An enhanced susceptibility to cell death was observed in BI-1 expressing cells after exposure to nutrient starvation (Figure 3E). Taken together, these data suggest a direct correlation between the effect of BI-1 expression on cell survival under nutrient starvation and the regulation of autophagy levels.

Activation of JNK mediates the enhancement of autophagy in BI-1-deficient cells

We monitored the phosphorylation of an mTOR target, as a direct measure of the nutrient starvation sensing activity regulating the TORC1 protein complex. A similar level of dephosphorylation of the mTOR target p70S6 kinase was observed in BI-1 WT and KO cells after stimulation with EBSS for 3 h (Figure 4A), indicating that BI-1 deficiency does not alter the ability of the cell to detect and initiate the response to starvation. JNK is a critical modulator of autophagy in different settings (Maundrell *et al*, 1997;

Pattingre *et al*, 2005, 2009; Wei *et al*, 2008a). Interestingly, it has been reported that *bi-1*-deficient mice show enhanced JNK phosphorylation in models of ischaemia reperfusion (Bailly-Maitre *et al*, 2006; Krajewska *et al*, 2011). To explore

a possible mechanism underlying the enhancement of autophagy levels in BI-1-deficient cells, we determined the levels of JNK phosphorylation in BI-1 WT and KO cells, and monitored changes in the kinetic of activation. We observed stronger



and sustained JNK phosphorylation in BI-1-deficient cells after stimulation with nutrient starvation when compared with control experiments (Figure 4C). We then treated cells with the specific JNK inhibitor SP600125 and studied LC3 parameters as an indicator of autophagy induction. Treatment of cells with SP600125 decreased the activation of JNK (Figure 4C) and the induction of LC3-II conversion in BI-1-deficient cells under nutrient starvation (Figure 4C). Similarly, the accumulation of LC3-positive vesicles in BI-1 KO cells was decreased by the treatment with SP600125 (Figure 4B; Supplementary Figure S3A).

JNK regulates autophagy in part by phosphorylating BCL-2, releasing Beclin-1 from this inhibitory interaction (Wei *et al*, 2008a). We monitored BCL-2 phosphorylation in BI-1 KO cells after exposure to nutrient deprivation. A marked shift in the electrophoresis pattern of BCL-2 was observed in BI-1-deficient cells when compared with control cells (Figure 4D). This phenomenon was partially reverted by treating cells with SP600125 (Figure 4D). As positive control for the electrophoretic shift, cells were treated with taxol, which induces JNK-dependent phosphorylation of BCL-2 (Supplementary Figure S3B; Bassik *et al*, 2004).

We then evaluated the impact of BI-1 on the stability of the Beclin-1/BCL-X_L complex under conditions of nutrient starvation. We transiently expressed a MYC tag construct of Beclin-1 together with a FLAG-tagged BCL-X_L. A faster dissociation of the Beclin-1/BCL-X_L complex was observed in BI-1 KO cells when compared with wild-type cells (Figure 4E). Since BI-1 physically interacts with BCL-2 and BCL-X_L (Xu and Reed, 1998; Lisbona *et al*, 2009), we performed additional experiments to evaluate if BI-1 interacts with Beclin-1 and BCL-X_L/BCL-2 complexes. Immunoprecipitation (IP) of Beclin-1-MYC confirmed the interaction of Beclin-1 with BCL-X_L (Figure 4F), but we did not observe any interaction between BI-1 and Beclin-1. In addition, we were able to co-IP BI-1-MYC with BCL-X_L-FLAG (Figure 4G), but no interaction with Beclin-1-FLAG was detected, suggesting that BCL-X_L could form distinct and independent complexes with BI-1 or Beclin-1.

To address the possible functional role of Beclin-1 in the control of autophagy downstream of BI-1, we knocked down Beclin-1 expression in BI-1-deficient cells. As shown in Figure 5A, decreasing Beclin-1 expression diminished the basal accumulation of LC3-II in BI-1 null cells. Similarly, the enhancement of autophagy by stimulation with EBSS was attenuated by knocking down Beclin-1, which was confirmed by monitoring LC3 distribution by immunofluor-

escence (Figure 5C; Supplementary Figure S3C). Thus, BI-1 deficiency triggers JNK/Beclin-1-dependent autophagy.

BI-1 negatively regulates IRE1 α -dependent autophagy

Based on the observation that BI-1 interacts and control the activity of IRE1 α (Lisbona *et al*, 2009) and IRE1 α regulates the activation of JNK under ER stress conditions (Urano *et al*, 2000), we monitored the possible contribution of IRE1 α to the regulation of autophagy by BI-1. We targeted IRE1 α mRNA with an shRNA construct in BI-1 KO cells. Knocking down IRE1 α decreased the basal levels of LC3-II in BI-1-deficient cells (Figure 5A), in addition to reduce the induction of LC3-II after nutrient starvation (Figure 5B and D; Supplementary Figure S3D). No significant changes on IRE1 α mRNA or protein levels were observed between BI-1 WT and KO cells (Supplementary Figure S1F).

IRE1 α interacts with the adaptor protein TRAF2 through its cytosolic region, leading to JNK activation (Urano *et al*, 2000; Nishitoh *et al*, 2002). Consistent with the effects of IRE1 α knockdown on autophagy levels in BI-1-deficient cells, transient expression of a dominant-negative form of TRAF2 reduced LC3-II levels at resting conditions and under nutrient starvation (Figure 5E). We then tested the possible impact of BI-1 on the binding of TRAF2 to IRE1 α using IP experiments. We transiently transfected 293T cells with HA-tagged IRE1 α , as well as a FLAG-tagged version of TRAF2, in the presence or absence of MYC-tagged BI-1. After IP of IRE1 α -HA, we detected the specific co-precipitation of TRAF2, which was significantly reduced by the expression of BI-1-MYC (Figure 5F). In addition, we monitored whether or not the interaction of BI-1 with IRE1 α is modulated by nutrient starvation. An enhanced association of BI-1-MYC with IRE1 α -HA was detected in cells exposed to EBSS media for 4 h (Supplementary Figure S3E). Together, these data suggest that the association of BI-1 with IRE1 α is dynamic and represses the binding of TRAF2 to the UP-osome, correlating with decreased JNK activation under starvation conditions.

BI-1 controls autophagy *in vivo* in mice and fly models

To validate the possible role of BI-1 in autophagy *in vivo*, we developed gain and loss of function approaches in *D. melanogaster*. Using the Gal4/UAS system (Brand and Perrimon, 1993), we targeted the expression of endogenous fly BI-1 (dBI-1) with a specific RNAi. This construct, together with the human LC3 fused to GFP (huLC3:GFP) (Rusten *et al*, 2004) and the RNase III Dicer-2 was ubiquitously co-expressed producing a highly efficient knockdown of dBI-1

Figure 4 BI-1 regulates Beclin-1-dependent autophagy by controlling JNK activation. (A) BI-1 WT and KO MEFs were treated with EBSS for 2 h, and the levels of phospho-p70S6k were determined by western blot analysis. Total p70S6k is also shown. (B) LC3 was monitored by immunofluorescence in cells treated with EBSS for 3 h in the presence or absence of 10 μ M JNK inhibitor SP600125. Mean and standard deviation are presented ($N=3$). Student's *t*-test was used to analyse statistical significance, * $P<0.001$ and ** $P<0.0001$. (C) BI-1 WT and KO cells were treated with EBSS for indicated time points, in the presence or absence of 10 μ M of the JNK inhibitor SP600125. Levels of phosphorylation of JNK (pJNK) and LC3-II were determined by western blot. The levels of total JNK and Hsp90 are shown as control ($N=4$). Image was assembled from cropped lanes of the same western blot analysis of the same gel. (D) BI-1 WT and KO cells were treated with EBSS for indicated time points in the presence or absence of 10 μ M SP600125, and the electrophoretic shift associated with BCL-2 phosphorylation was monitored by western blot. (E) BI-1 WT and KO cells were co-transfected with expression vectors for Beclin-1-MYC, BI-1-HA, and BCL-X_L-FLAG. After 24 h, cells were treated with EBSS for 2 h or left untreated. The association of MYC-tagged expressed Beclin-1 and BCL-X_L-FLAG was assessed by immunoprecipitation of Beclin-1 followed by western blot analysis. (F) 293T cells were co-transfected with expression vectors for Beclin-1-MYC, BI-1-HA, and BCL-X_L-FLAG. Cell extracts were prepared in CHAPS buffer and Beclin-1-MYC immunoprecipitated, and the possible co-precipitation of BI-1-HA, and BCL-X_L-FLAG was assessed by western blot analysis ($N=3$). Asterisks indicate BI-1 oligomers. (G) 293T cells were co-transfected as described in (F) and BI-1-HA was immunoprecipitated, and the possible co-precipitation of Beclin-1-MYC, and BCL-X_L-FLAG determined by western blot analysis ($N=3$). Figure source data can be found with the Supplementary Information.

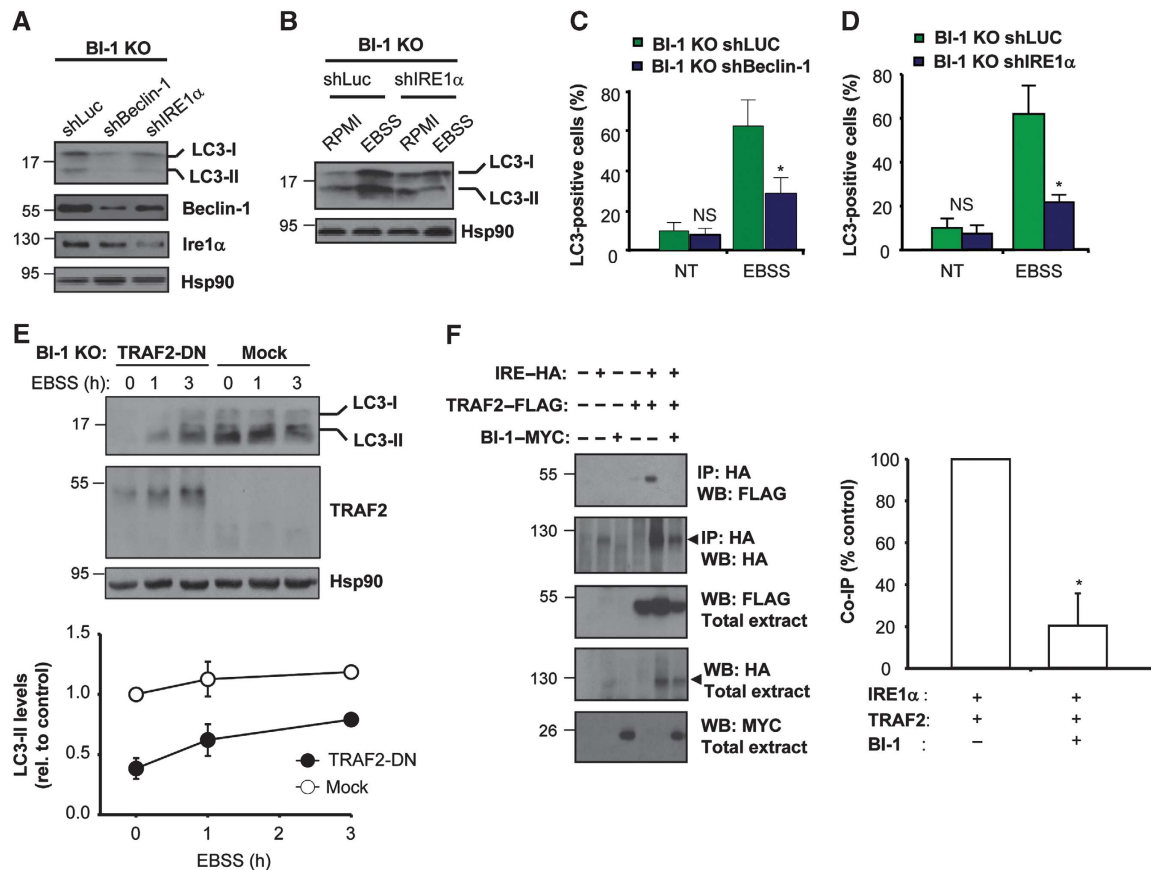


Figure 5 The regulation of nutrient starvation-induced autophagy by BI-1 depends on IRE1 α and TRAF2. (A) BI-1 KO MEFs were stably transduced with lentiviral vectors expressing an shRNA against *beclin-1* (shBeclin-1) or *ire1 α* (shIRE1 α) mRNA or *luciferase* (shLuc) as control. The levels of LC3, Beclin-1, IRE1 α and Hsp90 were monitored by western blot. (B) BI-1 KO MEFs were stably transduced with lentiviral vectors as described in A. Cells were exposed to EBSS for 3 h, and then LC3 levels were analysed by western blot. Image was assembled from cropped lanes of the same western blot analysis. (C) Endogenous LC3 distribution was visualized using immunofluorescence and confocal microscopy in BI-1 KO/shLuc and BI-1 KO/shBeclin-1 cells. Quantification represents the visualization of at least 180 cells. Student's *t*-test was used to analyse statistical significance. Mean and standard deviation are presented, **P* < 0.001, NS: non-significant. (D) LC3 was visualized and quantified in BI-1 KO/shLuc and BI-1 KO/shIRE1 α cells described in (B) by immunofluorescence and confocal microscopy analysis. (E) BI-1 KO cells were transiently transfected with a TRAF2 dominant-negative (TRAF2-DN) construct or empty vector (mock), and after 48 h cells were stimulated with EBSS and the levels of LC3-II and Hsp90 were monitored by western blot. Right panel: quantification of relative LC3-II levels normalized with Hsp90 and non-treated cells. Mean and standard deviation are presented. (F) 293T cells were co-transfected with expression vectors for HA-tagged IRE1 α (IRE1-HA), TRAF2-FLAG, and MYC-tagged BI-1 (BI1-MYC). After 48 h of transfection, HA-tagged proteins were immunoprecipitated and the possible interaction with TRAF2 was analysed by western blot. Right panel: the percentage of TRAF2 dissociation from IRE1 α by the presence or absence of BI-1 was quantified and normalized with the expression levels observed in the inputs. For comparison, the co-IP signal observed in the absence of BI-1 was normalized as 100% co-IP in each independent experiment (*N* = 3). Mean and standard deviation are presented, **P* < 0.05. Figure source data can be found with the Supplementary Information.

and the expression of human LC3:GFP fusion protein (Figure 6A and C). The levels of human LC3 were monitored in total tissue extracts by western blot analysis. Knocking down BI-1 led to a massive upregulation of LC3-II expression at basal levels and after exposure of fly larvae to nutrient starvation (Figure 6B). Furthermore, accumulation of LC3 in dBI-1 RNAi larvae was reduced by treatments with 100 μ M of SP600125 after 6 h of nutrient starvation (Figure 6B), confirming the requirement of JNK for the enhancement of autophagy levels by BI-1 deficiency.

The degradation of fly salivary gland during pupae development is a well-established model of autophagy *in vivo* (Berry and Baehrecke, 2007; Simon *et al*, 2009; Denton *et al*, 2010). To address the impact of dBI-1 expression on this physiological process, we evaluated in control and dBI-1 knockdown animals the appearance of LC3:GFP-positive dots, actin cytoskeleton structure, and tissue degradation

during salivary gland development. We monitored an early time point at 6 h after puparium formation (APF), when autophagy has not been induced yet in wild-type animals, and a late time point at 14 h APF when tissue has activated autophagy and partially degraded the salivary gland. We observed a marked accumulation of LC3:GFP-positive dots in the salivary gland of synchronized early dBI-1 RNAi pupae at 6 h APF compared with control animals, where ~75% of cells presented LC3-positive dots, whereas in control RNAi animals this phenomena was observed in <5% of the cells (Figure 6C, left panel). A faster elimination of salivary gland cells was observed in dBI-1 RNAi pupae, which was associated with enhanced cell shrinkage along with a decreased and disorganized pattern of rhodamine-phalloidin staining (Figure 6C, left panel).

We have recently characterized a mutant fly that overexpresses dBI-1 (dBI-1^{EY03662}) (Lisbona *et al*, 2009; Figure 6C,

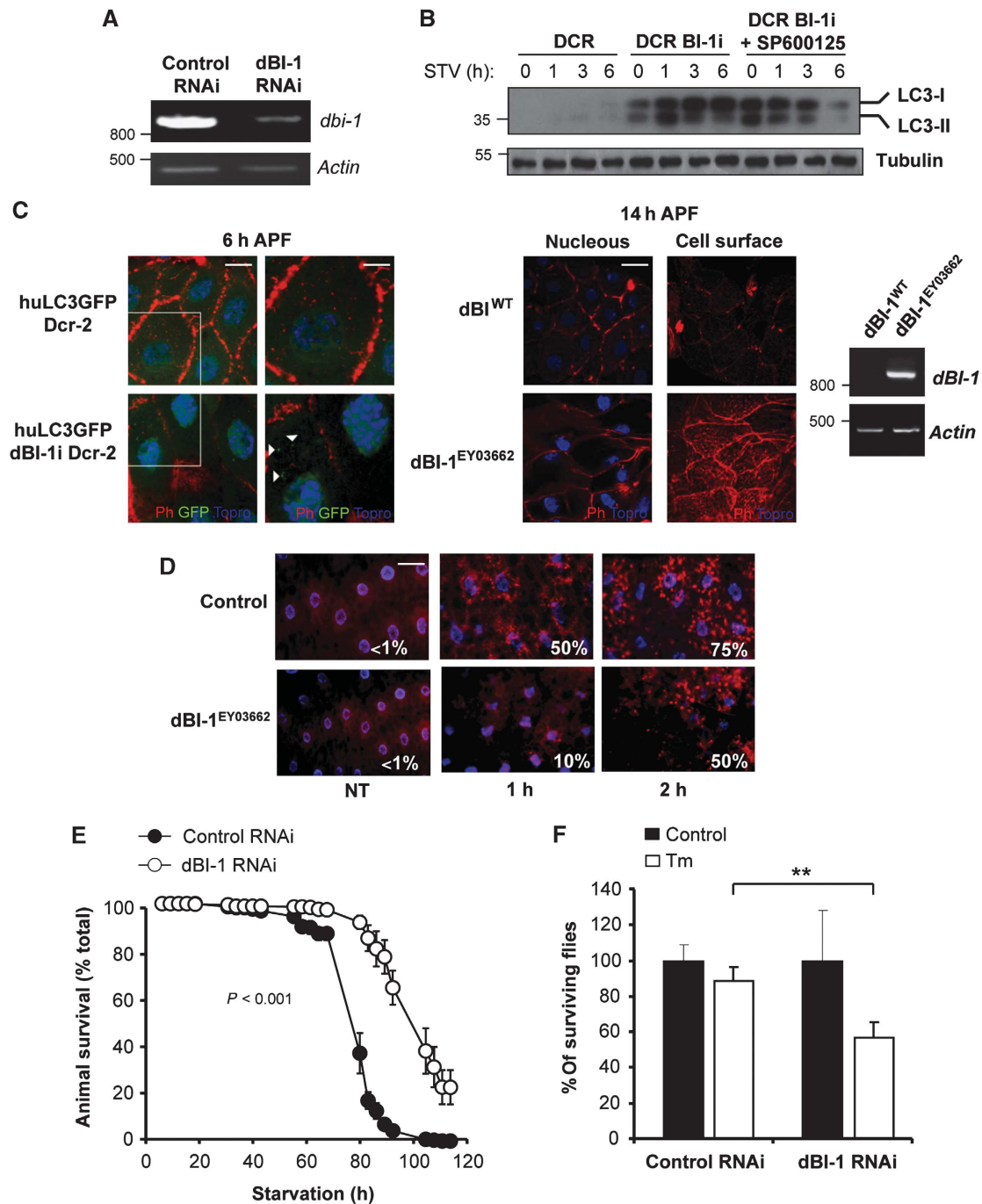


Figure 6 BI-1 controls autophagy activation *in vivo* in *Drosophila melanogaster*. (A) The expression of *dBi-1* was knocked down in *Drosophila melanogaster*. Then, relative expression levels of *dBi-1* mRNA were monitored by semiquantitative PCR. *Actin* levels were monitored as control. (B) LC3 levels were monitored in control (Da-Gal4 > huLC3:GFP) or *dBi-1* RNAi larvae (Da-Gal4 > huLC3:GFP, Dcr2, *dBi-1i*) under basal or fasting conditions. Then, huLC3-GFP levels were analysed by western blot. In addition, *dBi-1i* larvae were treated with 100 μ M SP600125 (added in the growing media). (C) Left panel: the presence of LC3-positive vesicles (white arrowheads) was monitored by confocal microscopy in control (Da-Gal4 > huLC3 > GFP) and *dBi-1* knockdown pupae (Da-Gal4 > huLC3:GFP, Dcr2, *dBi-1i*) after 6 h of puparium formation. The organization of actin cytoskeleton was monitored by staining with phalloidin (Ph, red). Nucleus was stained with Topro (blue). Scale bar: left 20 μ m and right 11 μ m. Right panel: overexpression of *dBi-1* (*dBi-1*^{EY03662}) delays salivary gland degradation. Overexpression of *dBi-1* was confirmed by semiquantitative RT-PCR. *Actin* levels were monitored as loading control. Right panel: wild-type control and *dBi-1*^{EY03662} pupae were analysed at 14 h after puparium formation. Superficial and internal confocal planes of the cells are presented. Scale bar: 40 μ m. (D) Wild-type control and *dBi-1*^{EY03662} larvae were cultured in fasting conditions for different periods of time and fat body stained with lysotracker (red) and Hoechst (blue). Then, lysosomal content in the fat body was visualized by epifluorescence microscopy. The percentage of cells presenting lysotracker-positive stain is indicated. Scale bar: 50 μ m. (E) Control or *dBi-1* knockdown adult flies were exposed to nutrient starvation and then animal viability was monitored over time for several days. In all, 100 individuals were monitored in each condition. Data represent mean and standard error ($N = 3$). Two-way ANOVA was used to analyse statistical significance between groups. (F) Second instar *dBi-1* RNAi or control larvae were grown in food supplemented with 25 μ g/ml Tm dissolved in DMSO or 0.5% DMSO as control. The number of individual reaching the adult fly stage was evaluated. Mean and standard error are presented ($N = 3$), ** $P < 0.01$.

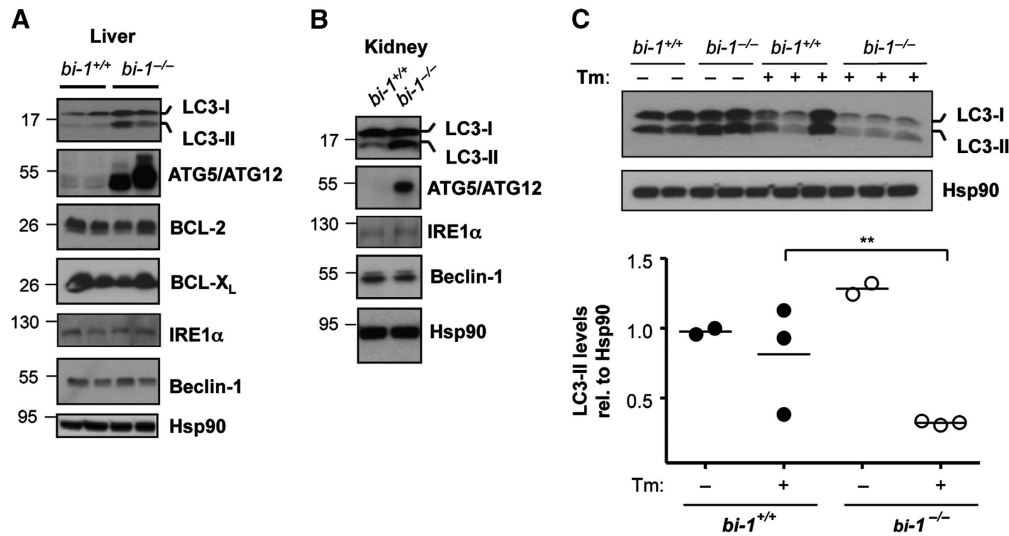


Figure 7 Enhanced LC3-II levels in the liver and kidney of *bi-1*-deficient mice. (A) The levels of LC3, Atg5/Atg12 complex, Beclin-1, Bcl-2, Bcl-X_L, IRE1 α and Hsp90 were monitored in liver protein extracts of *bi-1*^{+/+} and *bi-1*^{-/-} at 6-month-old mice. Each well represents independent mice. (B) A similar analysis was performed for indicated markers in kidney protein extracts as described in liver. (C) *bi-1*^{+/+} and *bi-1*^{-/-} mice were injected with 50 ng/ml of tunicamycin by intraperitoneal injection (*N* = 3) and then LC3 levels were monitored in liver protein extracts by western blot analysis. Right panel: quantification of relative LC3-II levels, ***P* < 0.005.

right panel). Consistent with the repressor activity of dBI-1 in autophagy induction, the actin cytoskeleton structure and morphological changes associated with the degradation of the salivary gland at 14 h APF were markedly delayed by the overexpression of dBI-1 (Figure 6C, right panel). This phenotype was reflected in an attenuated reduction on the cell size and the maintenance of phalloidin staining (Figure 6C). Using this dBI-1 overexpression fly model, we also visualized under fasting and control conditions the content of acidic compartments by lysotracker staining of the fat body, a tissue analogous to the liver and adipose tissue of mammals. Larvae overexpressing dBI-1 showed a marked delay in the accumulation of lysotracker-positive dots compared with control animals (Figure 6D). Visualization of LC3-GFP-positive vacuoles in dBI-1 knockdown larvae indicated an augmentation in the number of autophagosomes, in addition to increased number of lysosomes in the fat body of fasting larvae (Supplementary Figure S4A).

To further determine the impact of dBI-1 on adaptation to nutrient starvation, we fasted adult dBI-1 RNAi flies and then followed by animal survival over time. Remarkably, a substantial extension of fly lifespan was observed during nutrient starvation when we knocked down dBI-1 expression in the whole animal (Figure 6E; Supplementary Figure S4B). In contrast, treatment with the ER stress agent tunicamycin leads to decreased survival in dBI-1 RNAi animals when compared with the control RNAi strain (Figure 6F). Taken together, our results indicate an essential role of BI-1 in the control of autophagy levels *in vivo*.

Autophagy has a relevant role in maintaining basal liver and kidney function (Periyasamy-Thandavan *et al*, 2008; Jiang *et al*, 2010; Yang *et al*, 2010). For this reason, we also analysed the levels of autophagy markers in tissue derived from *bi-1*^{-/-} mice (Lisbona *et al*, 2009). We measured the levels of LC3 in liver tissue from 6-month-old mice and observed an increased expression of both LC3-I and LC3-II forms in *bi-1*^{-/-} mice when

compared with littermate control wild-type animals (Figure 7A). In agreement with this observation, a higher expression of the Atg5-Atg12 complex was observed in *bi-1*^{-/-} liver samples (Figure 7A). As control experiments, we monitored the expression levels of Bcl-2, Bcl-X_L, IRE1 α , and Beclin-1, and observed no significant differences in total protein levels between the studied genotypes (Figure 7A). Similarly, LC3-II levels and Atg5-Atg12 expression were markedly increased in *bi-1*^{-/-} kidney samples (Figure 7B). In order to monitor the relative levels autophagy fluxes *in vivo*, we stimulated autophagy by injecting *bi-1*^{-/-} mice with tunicamycin, which is a potent inducer of autophagy (Ogata *et al*, 2006; Yorimitsu *et al*, 2006; Criollo *et al*, 2007). Analysis of the extent of LC3-II degradation after intraperitoneal injection of a low dose of tunicamycin (50 ng/g mice) in *bi-1*^{-/-} and control wild-type littermate mice revealed higher amplitude of LC3-II degradation in the BI-1-deficient mice (Figure 7C). These results suggest that BI-1 expression modulates the level of basal and inducible autophagy *in vivo* in mice.

A putative yeast homologue of BI-1 has been identified, termed Ynl305c (Chae *et al*, 2003). To determine the possible function of Ynl305c in autophagy in yeast, we measured starvation-induced autophagy in wild-type and Δ Ynl305c cells using the established Pho8 Δ 60 assay (Noda *et al*, 1995; Noda and Klionsky, 2008). Pho8 Δ 60 is a cytoplasmic alkaline phosphatase that is kept inactive by an autoinhibitory propeptide until it is delivered into lysosomes by autophagy and the propeptide is cleaved off. As negative controls, we included cells lacking the key autophagy gene *ATG7* or the *PEP4* gene. We starved yeast of nitrogen for 9 h and measured the induction of alkaline phosphatase and did not find differences between wild-type and Δ Ynl305c cells (Supplementary Figure S5A-C). We corroborated these results using the GFP-Atg8 cleavage assay (Supplementary Figure S5D). These findings suggest that Ynl305c is dispensable for nutrient starvation-induced autophagy in yeast.

Discussion

Autophagy (self eating) and apoptosis (self killing) are interconnected processes, essential to maintain homeostasis during development and in adult tissue. Deregulation of these two pathways results in diverse pathological conditions including cancer, neurodegeneration, and many other diseases (Mizushima *et al*, 2008). Accumulating evidence suggests that apoptosis-regulatory proteins actually are part of distinct protein complexes with components of the core autophagy machinery in mammalian cells (Maiuri *et al*, 2007b; Ravikumar *et al*, 2010). Here, we provide evidence for a role of the anti-apoptotic protein BI-1 as a negative regulator of autophagy. A contrasting aspect of the interconnection between apoptosis and autophagy regulatory proteins is the fact that in most of the cases autophagy has an adaptive and pro-survival effect (Maiuri *et al*, 2007b; Ravikumar *et al*, 2010), which is blocked by several classical anti-apoptotic proteins (i.e., BCL-2 and BCL-X_L). Similarly, autophagy is engaged by pro-apoptotic factors (i.e., BH3-only proteins) (Mills *et al*, 2004; Pattingre *et al*, 2009; Stevens *et al*, 2009; Galluzzi *et al*, 2010; Yogev *et al*, 2010). This conundrum may actually represent an alternative function of apoptosis-related proteins beyond cell death in stress responses by the formation of distinct regulatory protein complexes. Similar examples have been described for several BCL-2 family members, where they modulate several stress responses (see reviews in Hetz and Glimcher, 2008 and Danial *et al*, 2010).

Although many members of the BCL-2 family of proteins have key functions in the regulation of mammalian autophagy, it is puzzling to notice that most of ATG-related proteins are actually highly conserved in other organisms such as flies, where only two putative BCL-2 family homologues have been identified. Phylogenetic analysis revealed that BI-1 is part of a family of proteins, the BI-1 family proteins, which is conserved across many multicellular organisms (Chae *et al*, 2003; Huckelhoven, 2004). BI-1 homologues are present in flies, plants, and yeast, with a conserved pro-survival activity against cell death (Chae *et al*, 2003; Bailly-Maitre *et al*, 2006; Reimers *et al*, 2008). Here, we explored the possible role of BI-1 in autophagy and observed that BI-1 deficiency leads to elevated LC3-II accumulation even at resting conditions, showing a faster and stronger activation of autophagy under nutrient starvation. Remarkably, dBI-1 expression modulated the degradation of the larvae salivary gland in *D. melanogaster*, a developmental process strictly dependent on autophagy and not on apoptosis (Berry and Baehrecke, 2007; Denton *et al*, 2010). More importantly, BI-1 deficiency in adult flies led to a significant enhancement of animal lifespan under fasting conditions. All these data together suggest a conserved autophagy inhibitory activity of BI-1.

The enhancement of autophagy observed in BI-1 KO cells is dependent on Beclin-1 expression and mediated by IRE1 α and JNK. These effects may be related to antagonizing TRAF2 binding to IRE1 α , enhancing JNK activation. Of note, autophagy stimuli did not induce XBP-1 mRNA splicing (not shown), despite the engagement of IRE1 α -dependent JNK phosphorylation. Interestingly, recent reports indicated that IRE1 α is specifically phosphorylated on Ser⁷²⁴ by glucose stimulation, and unlike the activation of IRE1 α by inducers of ER stress, glucose-induced phosphorylation did not cause

a shift of the IRE1 α protein as detected by western blot (Lipson *et al*, 2006; Qiu *et al*, 2010), and did not release the inhibitory interactions with BiP (Lipson *et al*, 2006). Moreover, modulation of Ser⁷²⁴ phosphorylation, as opposed to ER stress, does not trigger XBP-1 mRNA splicing (Qiu *et al*, 2010), consistent with our observations. Together with the current study, these data suggest that IRE1 α has a metabolic sensing activity with signalling outputs and regulatory aspects that are distinct from the events classically described under ER stress conditions.

Autophagy is becoming an emerging pathway relevant to the physiology of different organs, and alterations in the autophagy process contribute to the occurrence of several diseases (reviewed in Levine and Kroemer, 2008 and Ravikumar *et al*, 2010). The data presented here uncover a novel non-apoptotic function of BI-1, namely the control of autophagy. Together with our findings, a common denominator of the distinct functions identified so far for BI-1 emerges, where it operates as a specialized ‘stress integrator’ that modulates multiple adaptive responses against cellular insults. BI-1 may also participate in cell fate decisions when cell damage is deemed irreversible, and thus have a dual role. Based on the emerging cross talk between apoptosis and autophagy regulatory components, exploring the function of the TMBIM family may offer fundamental insights into conserved molecular mechanisms underlying adaptation to metabolic and protein folding stress.

Materials and methods

Materials

Tunicamycin (Tm) was purchased from Calbiochem EMB Bioscience Inc. Cell culture media, fetal bovine serum, and antibiotics were obtained from Life Technologies (MD, USA). Hoechst, LysoTracker, and ALEXA secondary antibodies were purchased from Molecular Probes (Eugene, OR). Bafilomycin A1, 3-methyladenine, E64D, and Pepstatin were provided by Sigma. EBSS and RPMI were purchased from Sigma (cat. #E2888 and R5886, respectively).

Western blot analysis

Cells were collected in RIPA buffer (20 mM Tris (pH 8.0), 150 mM NaCl, 0.1% SDS, 0.5% DOC, and 0.5% Triton X-100) containing a protease inhibitor cocktail obtained from Roche (Basel, Switzerland) as described before (Hetz *et al*, 2006). The following antibodies and dilutions were used: anti-LC3B 1:2000, anti-HSP90 1:5000, anti-Beclin 1:2000, anti-ATG5/12 1:1000, anti-pJNK 1:1000, anti-JNK 1:1000, anti-IRE1 α 1:1000 (Cell Signaling Technology), anti-phosphoIRE1 α 1:800 (Novus Biologicals), anti-p62/SQSTM1 1:10000 (Abcam), anti-BCL-2 1:1000 (BD Transduction Laboratories), and anti-GFP 1:3000, anti-TRAF-2 1:1000 (Santa Cruz Biotechnology).

Viability assay

To induce starvation, the culture medium was replaced by EBSS or glucose/serum-free RPMI starvation media for various time points. PI permeability was evaluated by flow cytometry (FACS Canto A, BD). For cell replating experiments, 3.0×10^5 cells were harvested in 3.5 cm dishes and treated with 1 μ g/ml of Tm for 4 h or exposed to EBSS or RPMI for 6 h. Cells were washed and then trypsinized. In all, 2×10^5 MEFs cells were replated into 10 cm dishes and cultured for 5 days in regular DMEN media and then stained with crystal violet.

RT-PCR and knockdowns

Real-time PCR assays were previously described (Lisbona *et al*, 2009). Primer sequence for LC3 as follow: forward 5'-CCCATCTCC GAAGTGTACGAG-3' and reverse 5'-TACAGGAAGCCGTCTTCATCT-3'. Primer sequence for p62 as follow: forward 5'-CGATGACTGGACA

CATTTGTCT-3' and reverse 5'-GTCCTTCCTGTGAGGGGCT-3'. We generated stable MEFs cells with reduced levels of BI-1, IRE1 α , and Beclin-1 as previously described (Hetz *et al*, 2007) by targeting the respective mRNA with shRNA using the lentiviral expression vector pLKO.1 and puromycin selection. As control, an shRNA construct against the *luciferase* gene was employed. Constructs were generated by The Broad Institute (Boston, MA). Targeting sequences identified for mouse BI-1, Beclin-1, and IRE1 α were 5'-CCTCTTTGATACTCAGCTCAT-3', 5'-CCAGGATGATGTCCACAGAA-3', and 5'-GCTCGTGAATTGATAGAGAAA-3', respectively (Hetz *et al*, 2009). To produce stable cell lines for reconstitution of BI-1 KO cells with human BI-1-GFP, we use retroviral expression of tagged protein with MSCV Retroviral Expression System (Clontech) and puromycin selection according to manufacturer's guidelines.

Immunoprecipitation

IP experiments were conducted in NP-40 0.2% (for Beclin-1 IP) or CHAPS buffer (1% CHAPS, 100 mM KCl, 50 mM Tris (pH 7.5), 50 mM NaF, 1 mM Na₃VO₄, 250 mM PMSF, and protease inhibitors) using antibody protein A/G complex (Santa Cruz), anti-HA antibody-agarose complexes (Roche), or anti-MYC antibody-agarose complexes (Upstate Technology) as described before (Hetz *et al*, 2006). To assess the interaction between IRE1 α and TRAF2, co-IP was performed using NP-40 buffer (0.2% NP-40, 100 mM KCl, 50 mM Tris (pH 7.5), 50 mM NaF, 1 mM Na₃VO₄, 250 mM PMSF, and protease inhibitors) (Yoneda *et al*, 2001).

Fluorescent labelling

Lysosomes were visualized by staining living cells with 50 nM lysotracker 30 min at 37°C and 5% CO₂. Cells were washed two times with cold PBS and then fixed for 30 min with 4% formaldehyde on ice. For correlative light-electron microscope analysis, living cells cultured in plastic coverslips bearing identification patterns were stained with 50 nM lysotracker for 30 min at 37°C and 5% CO₂. Cells were imaged in an inverted fluorescence microscope and then fixed and processed using standard techniques for EM as described (Barrientos *et al*, 2011). Using the identification patterns, cells imaged by fluorescent microscopy were re-identified in semithin Epon sections and thin sections of the corresponding cells were analysed and imaged by EM. LC3 distribution was visualized by indirect immunofluorescence as described before (Hetz *et al*, 2009). LC3-RFP-GFP tandem biosensor of autophagy process was transfected in BI-1 WT and KO cells using Lipofectamine LTX transfection system (Invitrogen).

Fly stocks and starvation treatments

The fly stocks used were Canton S, UAS-Dicer 2, UAS-dBI-1i (v3235, VDRC stock center), UAS-eGFP-huLC3; Da-Gal4 and dBI-1^{EY03662} (Lisbona *et al*, 2009). The UAS-eGFP-huLC3; Da-Gal4 line and UAS-Dicer 2, UAS-dBI-1i were obtained by standard genetic crosses. For salivary gland analysis, animals were aged following puparium formation and processed according to Martin and Baehrecke (2004).

For the starvation assays, Canton S or dBI-1^{EY03662} larvae were grown in standard media until they reached the wandering third larva stage, then 20 larvae were shifted to 0.4% agar-PBS media and cultured for 1–6 h. To monitor adult fly viability after nutrient starvation, animals were kept in standard medium with a 12-h dark/light cycle for 1 week. After this period, animals were transferred to vials with agar 1%. The number of dead flies was scored five times a day for 5 days. In survival experiments after

tunicamycin exposure, 100 s instar larvae were fed with food supplemented with 25 μ g/ml Tm or control DMSO.

Yeast strains and autophagy assay

Yeast strains were generated by homologous recombination using PCR products (Longtine *et al*, 1998; Janke *et al*, 2004). To monitor autophagy by GFP-Atg8 cleavage, W303 wild-type, *ynl305c::HIS3* and *atg7::kan* cells were transformed with plasmid pRS316-GFPAtg8, grown to logarithmic phase in SC-URA medium at 30°C, harvested by centrifugation, resuspended to OD₆₀₀ = 0.3 in nitrogen-free SD-N starvation medium, and grown for another 8 h and processed for western blotting using mouse anti-GFP antibodies 7.1/13.1 (Roche). To measure autophagy with the Pho8 Δ 60 alkaline phosphatase assay, a *pho13::HIS3 kan::pGPD-Pho8 Δ 60* strain was derived from wild-type W303 and served as a starting point to generate strains additionally lacking the *YNL305C*, *ATG7* or *PEP4* genes. Strains were grown to logarithmic phase in YPD medium at 30°C, harvested by centrifugation and resuspended to OD₆₀₀ = 0.3 in YPD (control) or nitrogen-free SD-N medium (starvation). One mmol/l PMSF was added to the *pep4* mutant to completely block lysosomal proteolysis. To measure non-selective autophagy, a Pho8 Δ 60 alkaline phosphatase assay was performed as described (Noda, 2008; Noda and Klionsky, 2008).

Tunicamycin injection in mice

bi-1^{+/+} and *bi-1*^{-/-} mice were given a single 50 ng/g body weight intraperitoneal injection of a 0.05 mg/ml suspension of Tm in 150 mM dextrose as we previously described (Hetz *et al*, 2006).

Supplementary data

Supplementary data are available at *The EMBO Journal* Online (<http://www.embojournal.org>).

Acknowledgements

We thank Peter Thielen, Cecilia Zuñiga, Fabián Yañez and Craig Wirth for technical assistant. We thank David Ron for providing IRE1 α -deficient cells, and Dr Laurie Glimcher and The Broad Institute (Boston, USA) for providing shRNA lentiviral constructs. We also thank Dr John Reed for kindly providing *bi-1*^{-/-}-derived tissue. We thank Monica Perez for excellent EM processing. This work was supported primarily by the FONDECYT no. 1100176, FONDAP grant no. 15010006, Millennium Institute no. P09-015-F (to CH) and FONDECYT no. 3100112 (to KC). In addition, we thank support by Alzheimer's Association, Michael J Fox Foundation for PD Research and ICGB (to CH); CONICYT Doctoral fellowship (DR-R, FL and MC), and FONDECYT no. 1100366 (AG), FONDECYT no. 1090272 (JS), FONDECYT no. 1070377, Millennium Nucleus no. P07-011-F (FC). SS thanks Human Frontier Science Program. PW is an investigator of the Howard Hughes Medical Institute.

Author contributions: KC and CH wrote the manuscript, conceived or designed the experiments, performed the experiments, analysed the data; FL, DRR, BC, MN, FC, CI, SS and AG conceived and designed the experiments, performed the experiments, analysed the data; PW and JS conceived or designed the experiments, analysed the data.

Conflict of interest

The authors declare that they have no conflict of interest.

References

- Ahn T, Yun CH, Kim HR, Chae HJ (2010) Cardioplin, phosphatidyserine, and BH4 domain of Bcl-2 family regulate Ca²⁺/H⁺ antiporter activity of human Bax inhibitor-1. *Cell Calcium* **47**: 387–396
- Arsham AM, Neufeld TP (2009) A genetic screen in *Drosophila* reveals novel cytoprotective functions of the autophagy-lysosome pathway. *PLoS One* **4**: e6068
- Bailly-Maitre B, Belgardt BF, Jordan SD, Coornaert B, von Freyend MJ, Kleinriders A, Mauer J, Cuddy M, Kress CL, Willmes D, Essig M, Hampel B, Protzer U, Reed JC, Bruning JC (2010) Hepatic Bax inhibitor-1 inhibits IRE1 α and protects from obesity-associated insulin resistance and glucose intolerance. *J Biol Chem* **285**: 6198–6207
- Bailly-Maitre B, Fondevila C, Kaldas F, Droin N, Luciano F, Ricci JE, Croxton R, Krajewska M, Zapata JM, Kupiec-Weglinski JW, Farmer D, Reed JC (2006) Cytoprotective gene bi-1 is required for intrinsic protection from endoplasmic reticulum stress and ischemia-reperfusion injury. *Proc Natl Acad Sci USA* **103**: 2809–2814
- Barrientos SA, Martinez NW, Yoo S, Jara JS, Zamorano S, Hetz C, Twiss JL, Alvarez J, Court FA (2011) Axonal degeneration is mediated by the mitochondrial permeability transition pore. *J Neurosci* **31**: 966–978

- Bassik MC, Scorrano L, Oakes SA, Pozzan T, Korsmeyer SJ (2004) Phosphorylation of BCL-2 regulates ER Ca^{2+} homeostasis and apoptosis. *EMBO J* **23**: 1207–1216
- Berry DL, Baehrecke EH (2007) Growth arrest and autophagy are required for salivary gland cell degradation in *Drosophila*. *Cell* **131**: 1137–1148
- Brand AH, Perrimon N (1993) Targeted gene expression as a means of altering cell fates and generating dominant phenotypes. *Development* **118**: 401–415
- Chae HJ, Ke N, Kim HR, Chen S, Godzik A, Dickman M, Reed JC (2003) Evolutionarily conserved cytoprotection provided by Bax Inhibitor-1 homologs from animals, plants, and yeast. *Gene* **323**: 101–113
- Chae HJ, Kim HR, Xu C, Bailly-Maitre B, Krajewska M, Krajewski S, Banares S, Cui J, Digicaylioglu M, Ke N, Kitada S, Monosov E, Thomas M, Kress CL, Babendure JR, Tsien RY, Lipton SA, Reed JC (2004) BI-1 regulates an apoptosis pathway linked to endoplasmic reticulum stress. *Mol Cell* **15**: 355–366
- Chen N, Debnath J (2010) Autophagy and tumorigenesis. *FEBS Lett* **584**: 1427–1435
- Criollo A, Maiuri MC, Tasdemir E, Vitale I, Fiebig AA, Andrews D, Molgo J, Diaz J, Lavandero S, Harper F, Pierron G, di Stefano D, Rizzuto R, Szabadkai G, Kroemer G (2007) Regulation of autophagy by the inositol trisphosphate receptor. *Cell Death Differ* **14**: 1029–1039
- Daniel NN, Gimenez-Cassina A, Tondera D (2010) Homeostatic functions of BCL-2 proteins beyond apoptosis. *Adv Exp Med Biol* **687**: 1–32
- Denton D, Shrivage B, Simin R, Baehrecke EH, Kumar S (2010) Larval midgut destruction in *Drosophila*: not dependent on caspases but suppressed by the loss of autophagy. *Autophagy* **6**: 163–165
- Ding WX, Ni HM, Gao W, Yoshimori T, Stolz DB, Ron D, Yin XM (2007) Linking of autophagy to ubiquitin-proteasome system is important for the regulation of endoplasmic reticulum stress and cell viability. *Am J Pathol* **171**: 513–524
- Dohm CP, Siedenberg S, Liman J, Esposito A, Wouters FS, Reed JC, Bahr M, Kermer P (2006) Bax inhibitor-1 protects neurons from oxygen-glucose deprivation. *J Mol Neurosci* **29**: 1–8
- Galindo KA, Lu WJ, Park JH, Abrams JM (2009) The Bax/Bak ortholog in *Drosophila*, Debcl, exerts limited control over programmed cell death. *Development* **136**: 275–283
- Galluzzi L, Morselli E, Kepp O, Maiuri MC, Kroemer G (2010) Defective autophagy control by the p53 rheostat in cancer. *Cell Cycle* **9**: 250–255
- He C, Klionsky DJ (2009) Regulation mechanisms and signaling pathways of autophagy. *Annu Rev Genet* **43**: 67–93
- He C, Levine B (2010) The Beclin 1 interactome. *Curr Opin Cell Biol* **22**: 140–149
- Hetz C, Bernasconi P, Fisher J, Lee AH, Bassik MC, Antonsson B, Brandt GS, Iwakoshi NN, Schinzel A, Glimcher LH, Korsmeyer SJ (2006) Proapoptotic BAX and BAK modulate the unfolded protein response by a direct interaction with IRE1alpha. *Science* **312**: 572–576
- Hetz C, Glimcher L (2008) The daily job of night killers: alternative roles of the BCL-2 family in organelle physiology. *Trends Cell Biol* **18**: 38–44
- Hetz C, Glimcher LH (2009) Fine-tuning of the unfolded protein response: Assembling the IRE1alpha interactome. *Mol Cell* **35**: 551–561
- Hetz C, Thielen P, Fisher J, Pasinelli P, Brown RH, Korsmeyer S, Glimcher L (2007) The proapoptotic BCL-2 family member BIM mediates motoneuron loss in a model of amyotrophic lateral sclerosis. *Cell Death Differ* **14**: 1386–1389
- Hetz C, Thielen P, Matus S, Nassif M, Court F, Kiffin R, Martinez G, Cuervo AM, Brown RH, Glimcher LH (2009) XBP-1 deficiency in the nervous system protects against amyotrophic lateral sclerosis by increasing autophagy. *Genes Dev* **23**: 2294–2306
- Hou YC, Chittaranjan S, Barbosa SG, McCall K, Gorski SM (2008) Effector caspase Dcp-1 and IAP protein Bruce regulate starvation-induced autophagy during *Drosophila melanogaster* oogenesis. *J Cell Biol* **182**: 1127–1139
- Hoyer-Hansen M, Jaattela M (2007) Connecting endoplasmic reticulum stress to autophagy by unfolded protein response and calcium. *Cell Death Differ* **14**: 1576–1582
- Huckelhoven R (2004) BAX Inhibitor-1, an ancient cell death suppressor in animals and plants with prokaryotic relatives. *Apoptosis* **9**: 299–307
- Janke C, Magiera MM, Rathfelder N, Taxis C, Reber S, Maekawa H, Moreno-Borchart A, Doenges G, Schwob E, Schiebel E, Knop M (2004) A versatile toolbox for PCR-based tagging of yeast genes: new fluorescent proteins, more markers and promoter substitution cassettes. *Yeast* **21**: 947–962
- Jiang M, Liu K, Luo J, Dong Z (2010) Autophagy is a renoprotective mechanism during *in vitro* hypoxia and *in vivo* ischemia-reperfusion injury. *Am J Pathol* **176**: 1181–1192
- Kim HR, Lee GH, Ha KC, Ahn T, Moon JY, Lee BJ, Cho SG, Kim S, Seo YR, Shin YJ, Chae SW, Reed JC, Chae HJ (2008) Bax Inhibitor-1 is a pH-dependent regulator of Ca^{2+} channel activity in the endoplasmic reticulum. *J Biol Chem* **283**: 15946–15955
- Klionsky DJ, Abeliovich H, Agostinis P, Agrawal DK, Aliev G, Askew DS, Baba M, Baehrecke EH, Bahr BA, Ballabio A, Bamber BA, Bassham DC, Bergamini E, Bi X, Biard-Piechaczyk M, Blum JS, Bredesen DE, Brodsky JL, Brumell JH, Brunk UT *et al* (2008) Guidelines for the use and interpretation of assays for monitoring autophagy in higher eukaryotes. *Autophagy* **4**: 151–175
- Korolchuk VI, Saiki S, Lichtenberg M, Siddiqi FH, Roberts EA, Imarisio S, Jahreis L, Sarkar S, Futter M, Menzies FM, O’Kane CJ, Deretic V, Rubinsztein DC (2011) Lysosomal positioning coordinates cellular nutrient responses. *Nat Cell Biol* **13**: 453–460
- Krajewska M, Xu L, Xu W, Krajewski S, Kress CL, Cui J, Yang L, Irie F, Yamaguchi Y, Lipton SA, Reed JC (2011) Endoplasmic reticulum protein BI-1 modulates unfolded protein response signaling and protects against stroke and traumatic brain injury. *Brain Res* **1370**: 227–237
- Levine B, Kroemer G (2008) Autophagy in the pathogenesis of disease. *Cell* **132**: 27–42
- Lipson KL, Fonseca SG, Ishigaki S, Nguyen LX, Foss E, Bortell R, Rossini AA, Urano F (2006) Regulation of insulin biosynthesis in pancreatic beta cells by an endoplasmic reticulum-resident protein kinase IRE1. *Cell Metab* **4**: 245–254
- Lisbona F, Rojas-Rivera D, Thielen P, Zamorano S, Todd D, Martinon F, Glavic A, Kress C, Lin JH, Walter P, Reed JC, Glimcher LH, Hetz C (2009) BAX inhibitor-1 is a negative regulator of the ER stress sensor IRE1alpha. *Mol Cell* **33**: 679–691
- Longtine MS, McKenzie III A, Demarini DJ, Shah NG, Wach A, Brachat A, Philippsen P, Pringle JR (1998) Additional modules for versatile and economical PCR-based gene deletion and modification in *Saccharomyces cerevisiae*. *Yeast* **14**: 953–961
- Maiuri MC, Le Toumelin G, Criollo A, Rain JC, Gautier F, Juin P, Tasdemir E, Pierron G, Troulinaki K, Tavernarakis N, Hickman JA, Geneste O, Kroemer G (2007a) Functional and physical interaction between Bcl-X(L) and a BH3-like domain in Beclin-1. *EMBO J* **26**: 2527–2539
- Maiuri MC, Zalckvar E, Kimchi A, Kroemer G (2007b) Self-eating and self-killing: crosstalk between autophagy and apoptosis. *Nat Rev Mol Cell Biol* **8**: 741–752
- Martin DN, Baehrecke EH (2004) Caspases function in autophagic programmed cell death in *Drosophila*. *Development* **131**: 275–284
- Maudrell K, Antonsson B, Magnenat E, Camps M, Muda M, Chabert C, Gillieron C, Boschert U, Vial-Knecht E, Martinou JC, Arkinstall S (1997) Bcl-2 undergoes phosphorylation by c-Jun N-terminal kinase/stress-activated protein kinases in the presence of the constitutively active GTP-binding protein Rac1. *J Biol Chem* **272**: 25238–25242
- Mills KR, Reginato M, Debnath J, Queenan B, Brugge JS (2004) Tumor necrosis factor-related apoptosis-inducing ligand (TRAIL) is required for induction of autophagy during lumen formation *in vitro*. *Proc Natl Acad Sci USA* **101**: 3438–3443
- Mizushima N, Levine B, Cuervo AM, Klionsky DJ (2008) Autophagy fights disease through cellular self-digestion. *Nature* **451**: 1069–1075
- Nishitoh H, Matsuzawa A, Tobiume K, Saegusa K, Takeda K, Inoue K, Hori S, Kakizuka A, Ichijo H (2002) ASK1 is essential for endoplasmic reticulum stress-induced neuronal cell death triggered by expanded polyglutamine repeats. *Genes Dev* **16**: 1345–1355
- Noda T (2008) Viability assays to monitor yeast autophagy. *Methods Enzymol* **451**: 27–32
- Noda T, Klionsky DJ (2008) The quantitative Pho8Delta60 assay of nonspecific autophagy. *Methods Enzymol* **451**: 33–42

- Noda T, Matsuura A, Wada Y, Ohsumi Y (1995) Novel system for monitoring autophagy in the yeast *Saccharomyces cerevisiae*. *Biochem Biophys Res Commun* **210**: 126–132
- Ogata M, Hino S, Saito A, Morikawa K, Kondo S, Kanemoto S, Murakami T, Taniguchi M, Tani I, Yoshinaga K, Shiosaka S, Hammarback JA, Urano F, Imaizumi K (2006) Autophagy is activated for cell survival after endoplasmic reticulum stress. *Mol Cell Biol* **26**: 9220–9231
- Pattingre S, Bauvy C, Carpentier S, Levade T, Levine B, Codogno P (2009) Role of JNK1-dependent Bcl-2 phosphorylation in ceramide-induced macroautophagy. *J Biol Chem* **284**: 2719–2728
- Pattingre S, Tassa A, Qu X, Garuti R, Liang XH, Mizushima N, Packer M, Schneider MD, Levine B (2005) Bcl-2 antiapoptotic proteins inhibit Beclin 1-dependent autophagy. *Cell* **122**: 927–939
- Periyasamy-Thandavan S, Jiang M, Wei Q, Smith R, Yin XM, Dong Z (2008) Autophagy is cytoprotective during cisplatin injury of renal proximal tubular cells. *Kidney Int* **74**: 631–640
- Qiu Y, Mao T, Zhang Y, Shao M, You J, Ding Q, Chen Y, Wu D, Xie D, Lin X, Gao X, Kaufman RJ, Li W, Liu Y (2010) A crucial role for RACK1 in the regulation of glucose-stimulated IRE1 α activation in pancreatic beta cells. *Sci Signal* **3**: ra7
- Quinn L, Coombe M, Mills K, Daish T, Colussi P, Kumar S, Richardson H (2003) Buffy, a *Drosophila* Bcl-2 protein, has anti-apoptotic and cell cycle inhibitory functions. *EMBO J* **22**: 3568–3579
- Ravikumar B, Sarkar S, Davies JE, Futter M, Garcia-Arencibia M, Green-Thompson ZW, Jimenez-Sanchez M, Korolchuk VI, Lichtenberg M, Luo S, Massey DC, Menzies FM, Moreau K, Narayanan U, Renna M, Siddiqi FH, Underwood BR, Winslow AR, Rubinsztein DC (2010) Regulation of mammalian autophagy in physiology and pathophysiology. *Physiol Rev* **90**: 1383–1435
- Reimers K, Choi CY, Bucan V, Vogt PM (2008) The Bax Inhibitor-1 (BI-1) family in apoptosis and tumorigenesis. *Curr Mol Med* **8**: 148–156
- Ron D, Walter P (2007) Signal integration in the endoplasmic reticulum unfolded protein response. *Nat Rev Mol Cell Biol* **8**: 519–529
- Rusten TE, Lindmo K, Juhasz G, Sass M, Seglen PO, Brech A, Stenmark H (2004) Programmed autophagy in the *Drosophila* fat body is induced by ecdysone through regulation of the PI3K pathway. *Dev Cell* **7**: 179–192
- Settembre C, Di Malta C, Polito VA, Arcencibia MG, Vetrini F, Erdin S, Erdin SU, Huynh T, Medina D, Colella P, Sardiello M, Rubinsztein DC, Ballabio A (2011) TFEB links autophagy to lysosomal biogenesis. *Science* **332**: 1429–1433
- Sevrioukov EA, Burr J, Huang EW, Assi HH, Monserrate JP, Purves DC, Wu JN, Song EJ, Brachmann CB (2007) *Drosophila* Bcl-2 proteins participate in stress-induced apoptosis, but are not required for normal development. *Genesis* **45**: 184–193
- Simon CR, Moda LM, Octacilio-Silva S, Anhezini L, Machado-Gitai LC, Ramos RG (2009) Precise temporal regulation of roughest is required for correct salivary gland autophagic cell death in *Drosophila*. *Genesis* **47**: 492–504
- Stevens C, Lin Y, Harrison B, Burch L, Ridgway RA, Sansom O, Hupp T (2009) Peptide combinatorial libraries identify TSC2 as a death-associated protein kinase (DAPK) death domain-binding protein and reveal a stimulatory role for DAPK in mTORC1 signaling. *J Biol Chem* **284**: 334–344
- Tanida I, Ueno T, Kominami E (2008) LC3 and autophagy. *Methods Mol Biol* **445**: 77–88
- Urano F, Wang X, Bertolotti A, Zhang Y, Chung P, Harding HP, Ron D (2000) Coupling of stress in the ER to activation of JNK protein kinases by transmembrane protein kinase IRE1. *Science* **287**: 664–666
- Wei Y, Pattingre S, Sinha S, Bassik M, Levine B (2008a) JNK1-mediated phosphorylation of Bcl-2 regulates starvation-induced autophagy. *Mol Cell* **30**: 678–688
- Wei Y, Sinha S, Levine B (2008b) Dual role of JNK1-mediated phosphorylation of Bcl-2 in autophagy and apoptosis regulation. *Autophagy* **4**: 949–951
- Westphalen BC, Wessig J, Leypoldt F, Arnold S, Methner A (2005) BI-1 protects cells from oxygen glucose deprivation by reducing the calcium content of the endoplasmic reticulum. *Cell Death Differ* **12**: 304–306
- Wong E, Cuervo AM (2010) Autophagy gone awry in neurodegenerative diseases. *Nat Neurosci* **13**: 805–811
- Wu JN, Nguyen N, Aghazarian M, Tan Y, Sevrioukov EA, Mabuchi M, Tang W, Monserrate JP, White K, Brachmann CB (2010) grim promotes programmed cell death of *Drosophila* microchaete glial cells. *Mech Dev* **127**: 407–417
- Xu C, Xu W, Palmer AE, Reed JC (2008) BI-1 regulates endoplasmic reticulum Ca²⁺ homeostasis downstream of Bcl-2 family proteins. *J Biol Chem* **283**: 11477–11484
- Xu Q, Reed JC (1998) Bax inhibitor-1, a mammalian apoptosis suppressor identified by functional screening in yeast. *Mol Cell* **1**: 337–346
- Yang L, Li P, Fu S, Calay ES, Hotamisligil GS (2010) Defective hepatic autophagy in obesity promotes ER stress and causes insulin resistance. *Cell Metab* **11**: 467–478
- Yogev O, Goldberg R, Anzi S, Yogev O, Shaulian E (2010) Jun proteins are starvation-regulated inhibitors of autophagy. *Cancer Res* **70**: 2318–2327
- Yoneda T, Imaizumi K, Oono K, Yui D, Gomi F, Katayama T, Tohyama M (2001) Activation of caspase-12, an endoplasmic reticulum (ER) resident caspase, through tumor necrosis factor receptor-associated factor 2-dependent mechanism in response to the ER stress. *J Biol Chem* **276**: 13935–13940
- Yorimitsu T, Nair U, Yang Z, Klionsky DJ (2006) Endoplasmic reticulum stress triggers autophagy. *J Biol Chem* **281**: 30299–30304